DOUBLE PATH-INTEGRAL MIGRATION VELOCITY ANALYSIS: A REAL DATA EXAMPLE

J.C. Costa and J. Schleicher

email: *js@ime.unicamp.br*
keywords: *MVA, path integral, double stack, velocities, imaging*

ABSTRACT

Path-integral imaging forms an image with no knowledge of the velocity model by summing over the migrated images obtained for a set of migration velocity models. Double path-integral imaging migration extracts the stationary velocities, i.e., those velocities at which common-image gathers align horizontally, as a byproduct. An application of the technique to a real data set demonstrates that quantitative information about the migration velocity model can be determined by double path-integral migration velocity analysis. Migrated images using interpolations with different regularisations of the extracted velocities prove the high quality of the resulting velocity information. The so-obtained velocity model can then be used as a starting model for subsequent velocity analysis tools like migration velocity analysis or tomographic methods.

INTRODUCTION

To overcome the dependency of conventional imaging methods on the knowledge of a velocity model, Keydar (2004) and Landa (2004) have proposed a path-integral approach to seismic imaging. Its idea is to sum over the migrated images obtained for a set of migration velocity models. Those velocities where common-image gathers align horizontally are stationary, thus favouring these images in the overall stack. In this way, the overall image forms with no need to know the true velocity model.

Keydar (2004) applied the technique to inversion by homeomorphic imaging, which is based on an normal-moveout (NMO) correction formula represented as a function of certain wavefront parameters (radii of curvature and emergence angle), similar to the common-reflection-surface (CRS) method (see, e.g., Hertweck et al., 2007). Landa (2004) extended the idea to time migration. He proposed to obtain the subsurface seismic image by a summation of seismic signals over a representative sample of all possible paths/trajectories between a source and observation point. First applications of path-summation imaging in depth migration were presented by Landa et al. (2005) and Shtivelman and Keydar (2005). A similar idea was recently used by Anikiev et al. (2007) to locate seismic events in an unknown velocity field.

Landa et al. (2006) discuss path-summation imaging in more conceptual and theoretical detail. They stress that for path-summation imaging to be successful, the argument of the path integral must be chosen adequately, the integration must be carried out over a representative sample of all possible trajectories, and a properly designed weight function must be applied in the multipath summation. Particularly important is the weight function. It makes up for deficiencies in the model space sampling, since however fine we sample, there is no way of covering the model space it completely. A successful weight function was discussed by Keydar et al. (2008).

The beauty of the multipath summation method is that it eliminates the need to construct a migration velocity model before imaging. The multipath stack itself takes care of enhancing the true image as the only one that interferes constructively with images from slightly perturbed models. However, this very beauty turns into a drawback when the actual velocity model that is associated with the resulting image is needed, as is the case in many seismic applications. To overcome this problem, Schleicher and Costa

(2008) proposed last a method how the multipath summation can be modified to extract a meaningful velocity model together with the final image. By executing the path-integral imaging twice and weighting one of the stacks with the used velocity value, the stationary velocities that produce the final image can then be extracted by a division of the two images. In this paper, we apply this technique to a real data set. to demonstrate that quantitative information about the migration velocity model can be determined by double path-integral migration velocity analysis. Migrated images using interpolations with different regularisations of the extracted velocities prove the high quality of the resulting velocity information. The so-obtained velocity model can then be used as a starting model for subsequent velocity analysis tools like migration velocity analysis or tomographic methods.

DOUBLE PATH-INTEGRAL MIGRATION VELOCITY ANALYSIS

In this section, we briefly review the theory of double path-integral migration velocity analysis as discussed by Schleicher and Costa (2008). In the notation of Landa et al. (2006), the multipath-summation time-migration operator can be written as

$$V_W(\mathbf{x}) = \int d\alpha \, w(\mathbf{x}, \alpha) \int d\xi \int dt \, U(t, \xi) \delta(t - t_d(\xi, \mathbf{x}; \alpha)) \,, \tag{1}$$

where V_W is the resulting time-migrated image at an image point with coordinates $\mathbf{x} = (x, \tau)$, x being lateral distance and τ vertical time. In integral (1), $U(t, \xi)$ denotes a seismic trace at coordinate ξ in the seismic data, and $t_d(\xi, \mathbf{x}; \alpha)$ is a set of stacking surfaces corresponding to a set of possible velocity models α. Note that generally, the migration velocity α is a function of the position $\mathbf{x}$ of the image point, i.e., $\alpha = \alpha(\mathbf{x})$. The integration is weighted by a weight function $w(\mathbf{x}, \alpha)$, which is designed to attenuate contributions from unlikely trajectories and emphasise contributions from trajectories close to the optimal one. There are several possible choices for $w(\mathbf{x}, \alpha)$. Here, we follow the choice of Schleicher and Costa (2008), who opted for an exponential weight function of the form

$$w(\mathbf{x}, \alpha) = \exp[-P(\mathbf{x}; \alpha)/\sigma^2] \,, \tag{2}$$

where $P(\mathbf{x}; \alpha)$ is the squared average of the absolute value of the local event slopes in the common-image gather (CIG) at $\mathbf{x}$. The local event slopes are estimated using corrected least-square plane-wave filters as described in Schleicher et al. (2009). Parameter σ adjusts the half-width of the Gaussian bell function away from the desired events with $P = 0$. In our implementation, we chose $\sigma = 0.1\Delta\tau/\Delta x$.

Using Laplace's method (see, e.g., Erdélyi, 1956), integral (1) can be asymptotically evaluated to yield

$$V_W(\mathbf{x}) \approx \sqrt{\frac{2\pi\sigma^2}{P''(\alpha_0)}} Q_0(\mathbf{x}; \alpha_0) \,, \tag{3}$$

where the stationary value α_0 corresponds to the maximum of the weight function at $P = 0$, i.e., α_0 represents the best possible migration velocity. Moreover, $P''(\alpha_0)$ denotes the second derivative of P with respect to α. Finally, $Q_0(\mathbf{x}; \alpha_0)$ denotes the desired migration result with the stationary migration velocity α_0 [see also Landa et al. (2006)], viz.,

$$Q_0(\mathbf{x}; \alpha_0) = \int d\xi \int dt \, U(t, \xi) \delta(t - t_d(\xi, \mathbf{x}; \alpha_0)) \,. \tag{4}$$

The observation that the summation result (4) is proportional to the desired image implies that the use of a slightly modified weight function (Schleicher and Costa, 2008),

$$\tilde{w}(\mathbf{x}, \alpha) = \alpha \exp(-P((\mathbf{x}, \alpha)/\sigma^2) \,, \tag{5}$$

will lead to a slightly modified migration result,

$$\tilde{V}_W(\mathbf{x}) \approx \alpha_0 \sqrt{\frac{2\pi\sigma^2}{P''(\alpha_0)}} Q_0(\alpha_0) \,. \tag{6}$$
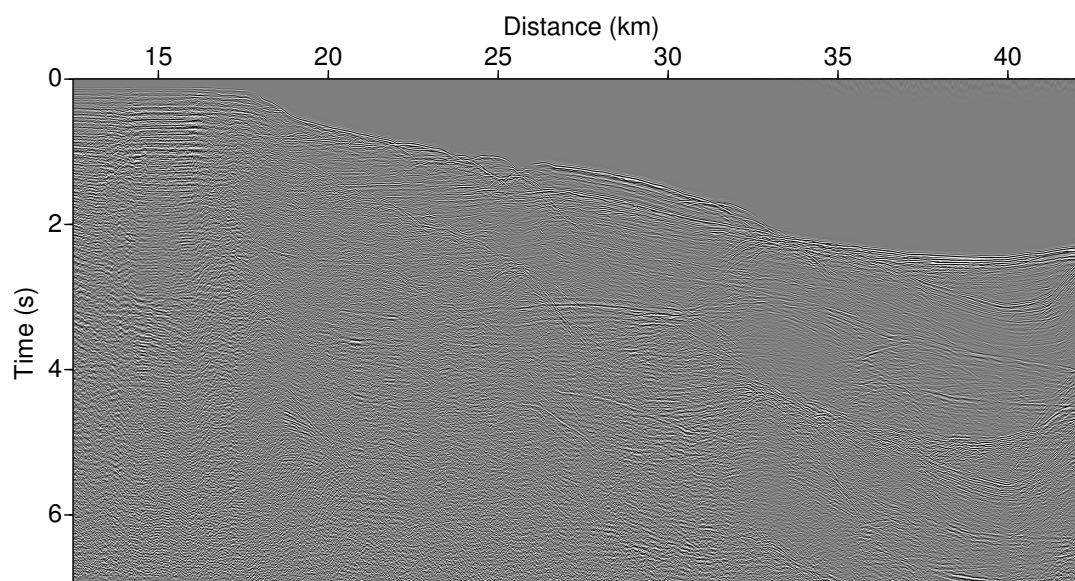
Figure 1: Near-offset section with source-receiver offset 150 m of the Jequitinhonha data set.

In other words, results (3) and (6) differ only by a constant factor, this factor being the true migration velocity at $\mathbf{x}$.

This readily suggests that the migration velocity can be extracted from such a procedure by simply dividing the two migration results (3) and (6), i.e.,

$$\alpha_0 \approx \frac{\tilde{V}_W(\mathbf{x})}{V_W(\mathbf{x})} \ . \tag{7}$$

In fact, this idea of extracting quantities from multiple stacks is not new but has already been previously discussed in the framework of Kirchhoff migration (Bleistein, 1987; Tygel et al., 1993).

Of course, since the image in the denominator will vanish off actual reflector images, care has to be taken to avoid division by zero. Schleicher and Costa (2008) showed that a reasonable way to avoid problems in this respect is to mask the division so that it is carried out only at points where the denominator exceeds a certain threshold value. Moreover, velocity values outside the range of velocities used in the path-integral summation should also be discarded.

A REAL DATA EXAMPLE

We have applied the double path-integral migration velocity analysis briefly reviewed above to a real data set. The data were acquired in 1985 by Petrobras in the Jequitinhonha basin offshore Brazil. They represent a single seismic line covering 39.4 km with 1578 shots at every 25 m and 120 channels, with offsets ranging from 150 m to 3125 m in steps of 25 m, recorded to a maximum time of 7 s. This gives rise to 2393 CMPs at every 12.5 m. Figure 1 depicts a near-offset section of these data after application of surface-related multiple elimination (SRME) and automatic gain control (AGC).

The result of the path-integral migration stack for a range of velocities between 1400 m/s and 4500 m/s in steps of 25 m/s are shown in Figure 2. Most of the features of the continental slope are nicely visible in this fully automatically obtained image.

Figure 3 shows the result of the velocity extraction using double path-integral migration velocity analysis. Note that zero values where attributed to every point where the denominator in equation (7) was below a threshold value of one thousandth of the maximum amplitude in Figure 2. Moreover, all velocity values outside the range of velocities used for the path-integral migration stack were zeroed after the division. Finally, zero velocity was attributed above the sea bottom, which was determined from interpretation of the migrated image with constant water velocity of 1500 m/s.
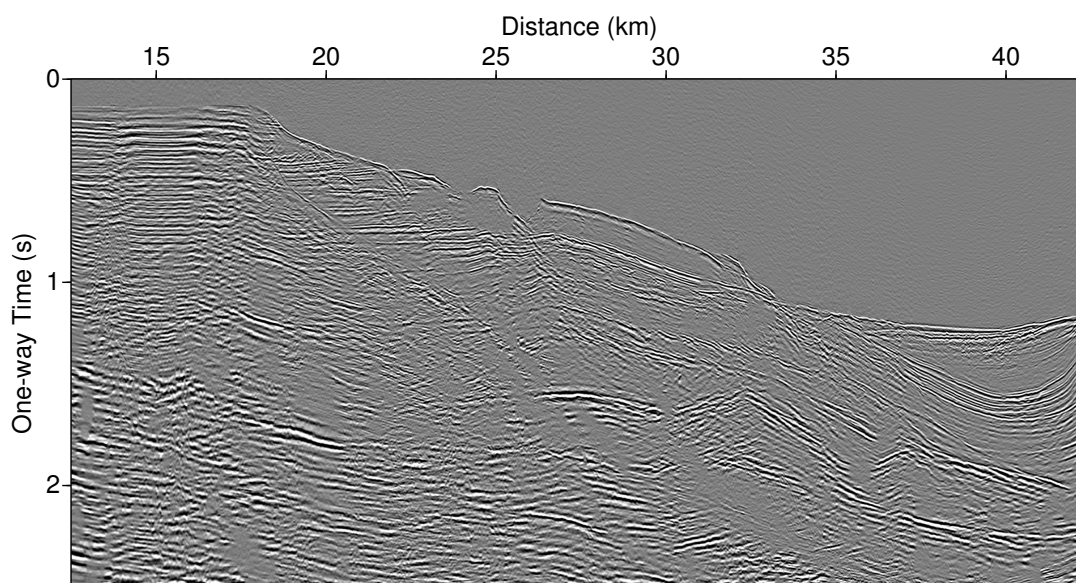
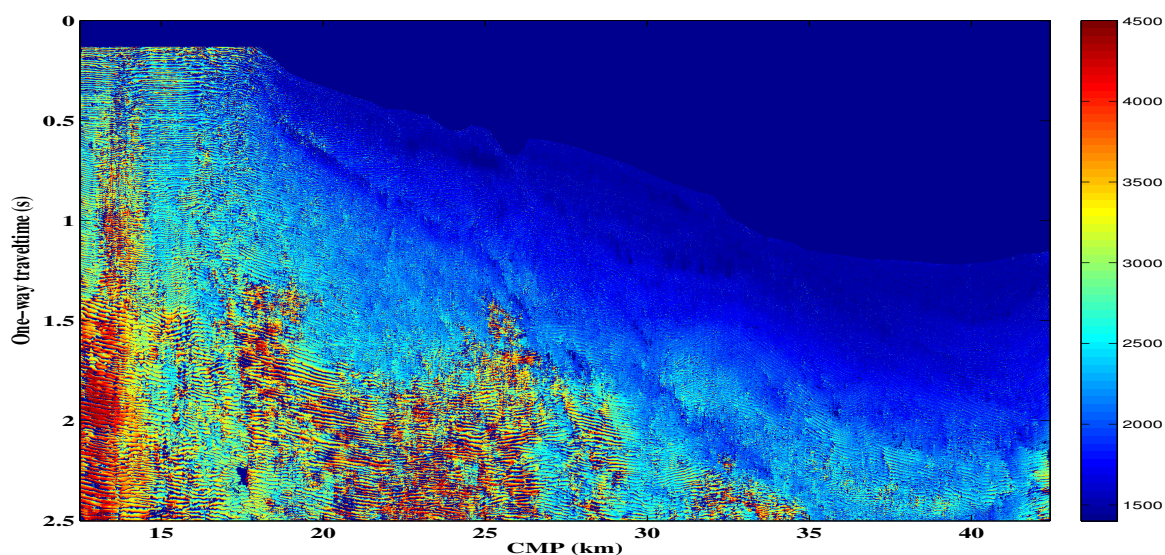**Figure 2:** Path-integral migration stack for the Jequitinhonha data set.

Figure 3: Velocities from double path-integral migration velocity analysis for the Jequitinhonha data set.

These extracted velocity values where subjected to different type of smoothing and interpolation. We started with filling the velocity values above the sea bottom with the water velocity of 1500 m/s. Next, we passed four times a zero-ignoring moving average filter with a window size of 25 time samples and 17 traces. The resulting velocity model had no longer any holes in it. We used these velocity values as input to B-splines smoothing on a grid with 36×63 nodes, i.e., with node spacing of 0.1 s and 500 m. The B-splines smoothing used minimum Cartesian derivative constraints. In the next set of figures, we show the resulting velocity models of this smoothing using three different Lagrangian multipliers, together with the corresponding time-migrated images.

The first set of figures was generated using the strongest regularisation, with Lagrangian multipliers of $\lambda_t = 10^{-3}$ for the time derivative, $\lambda_x = 2 \times 10^{-3}$ for the horizontal derivative, and $\lambda_{tt} = \lambda_{xx} = 10^{-4}$ for the second derivatives. Figure 4 shows the resulting velocity model and Figure 5 the corresponding
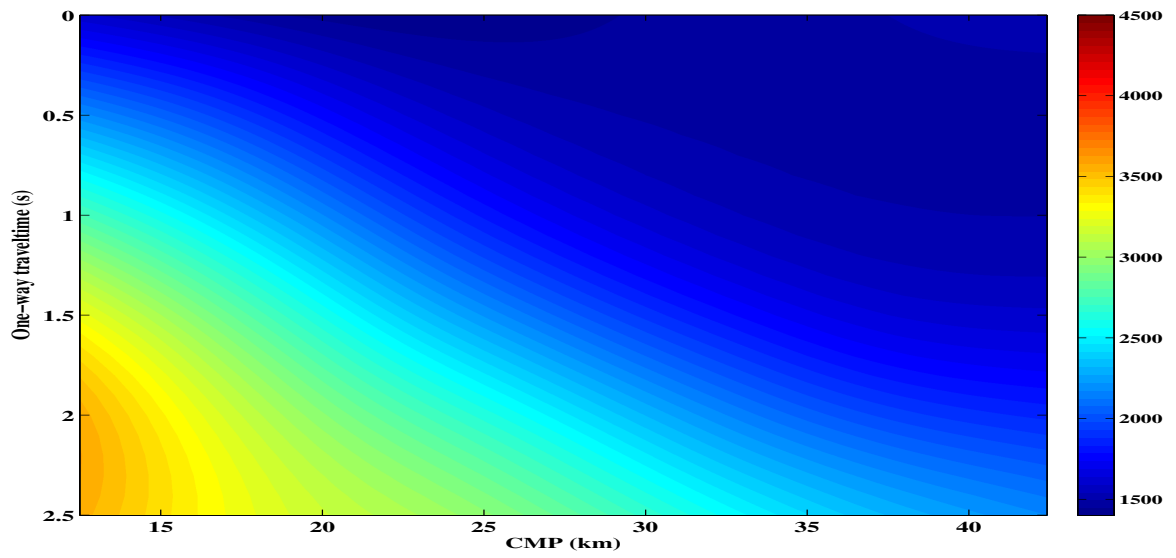
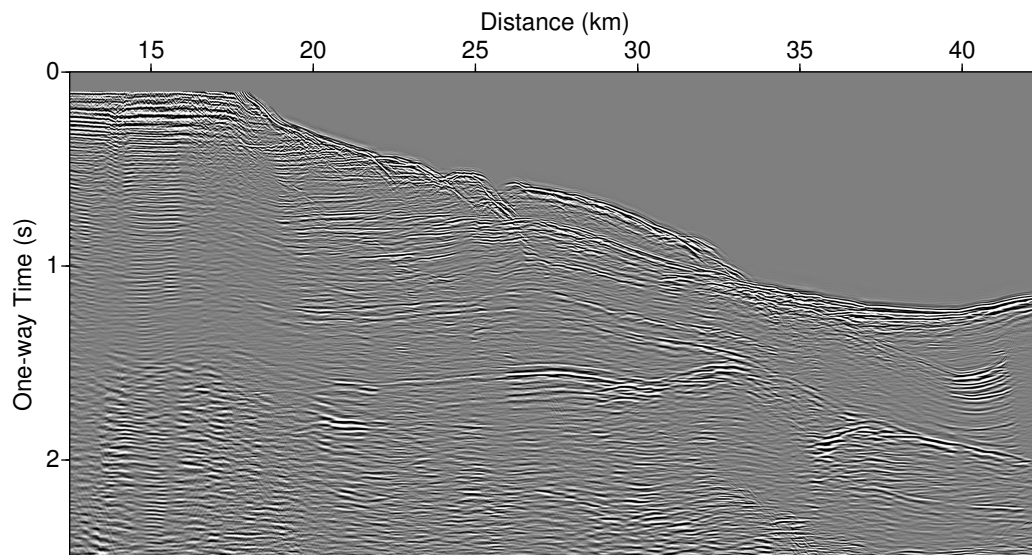**Figure 4:** Velocity model after smoothing with strong regularisation.

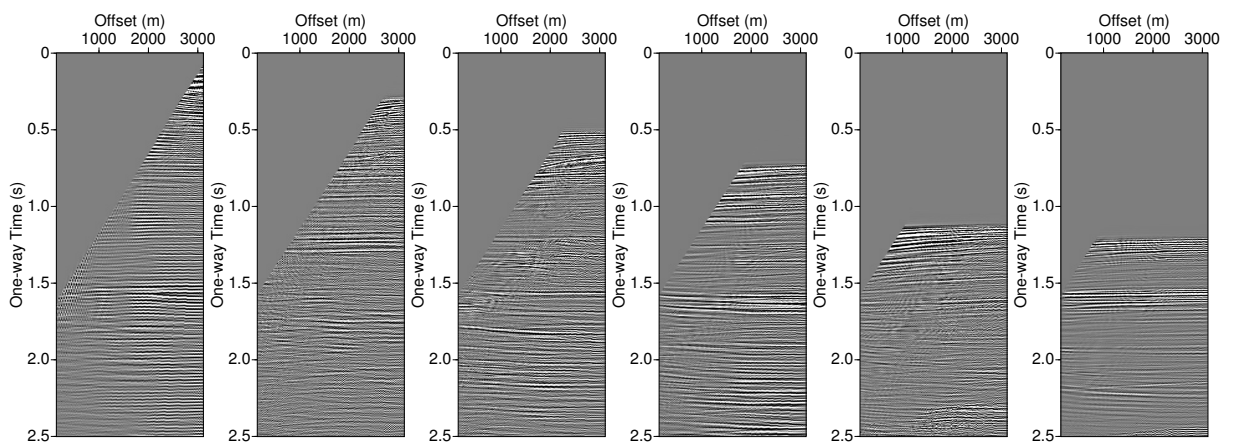**Figure 5:** Time-migration with strongly regularised velocity model.

Figure 6: Time-migration common-image gathers with strongly regularised velocity model.

time-migrated section. We see that this rather strong smoothing only preserves the general velocity trend and eliminates almost all local detail. The time-migrated image reproduces the most important features of the region. Figure 6 shows selected common-image gathers associated with this migration. While the overall impression is that these gathers are nicely flat, closer inspection reveals that some events still show a slight residual moveout. This might be an indication that a single velocity field is not sufficient to correctly position all events, particular in a 2D section covering a 3D setting. Another possible explanation are the general problems of time migration in laterally varying models.

The regularisation for the second set of figures was intermediate, the Lagrangian multipliers being three orders of magnitude lower than in the first example, i.e., $\lambda_t = 10^{-6}$, $\lambda_x = 2 \times 10^{-6}$, and $\lambda_{tt} = \lambda_{xx} = 2.5 \times 10^{-7}$. The resulting velocity model and time-migrated image are depicted in Figures 7 and 8, respectively. While some more local features of the velocity model are preserved with this intermediate regularisation, the effect on the time-migrated image is more harder to notice. Only at some isolated points of the image, small differences to the previous images can be noted. For example, the events in the centre of the image seem to lose some focusing. On the other hand, the trough-shaped reflector at the right side of the image comes better in focus now. The corresponding common-image gathers are shown in Figure 9. Some changes in the event flatness over the gathers in Figure 6 can be observed, though not always to the better. While some events appear to have been better flattened, there are others whose exhibit a stronger residual moveout.

The final set of figures was generated using the weakest regularisation, with Lagrangian multipliers $\lambda_t = 10^{-10}$, $\lambda_x = 10^{-10}$, and $\lambda_{tt} = \lambda_{xx} = 2.5 \times 10^{-11}$. The resulting velocity model and time-migrated image are depicted in Figures 10 and 11, respectively. This very weak regularisation preserves almost all details of the original velocity distribution. In spite of the clearly visible differences in the velocity models, the time-migrated image is hardly distinguishable from the one obtained with intermediate smoothing. Finally, Figure 12 shows the corresponding common-image gathers for this migration. Correspondingly to the migrated images, it is hard to spot a difference between these common-image gathers and those of Figure 9.

CONCLUSIONS

The idea of path-integral imaging is to sum over the migrated images obtained for a set of migration velocities. Those velocities where common-image gathers align horizontally are stationary, thus favouring these images in the overall stack. Other CIGs cancel each other in the final stack. An exponential weight function using the event slopes in the CIGs helps to enhance the constructive interference and to reduce undesired events that might not be completely cancelled by destructive interference.

By executing the path-integral imaging a second time with a modified weight function including the migration velocity as an additional factor and dividing the two resulting images, the stationary velocities that produce the final image can be extracted in the process. Since multipath-summation imaging does not rely on any kind of interpretation, this technique allows for the fully automated construction of a first time-migrated image together with a first time-migration velocity model that can then be used as a starting model for subsequent velocity analysis tools like migration velocity analysis or tomographic methods.

In this work, we have applied the technique to a real data set. In our numerical examples, final time-migrations using the extracted velocities resulted in nicely flattened image gathers. In this way, we have demonstrated that meaningful information about the migration velocity can be extracted from such a double path-integral migration velocity analysis. Moreover, we have compared the application of different degrees of smoothing to the extracted velocity. Stronger smoothing preserves only the general background trend of the velocity model, while weaker smoothing carries local details over to the final velocity model. The influence of the different degrees of smoothing on the final migrated images is much weaker.
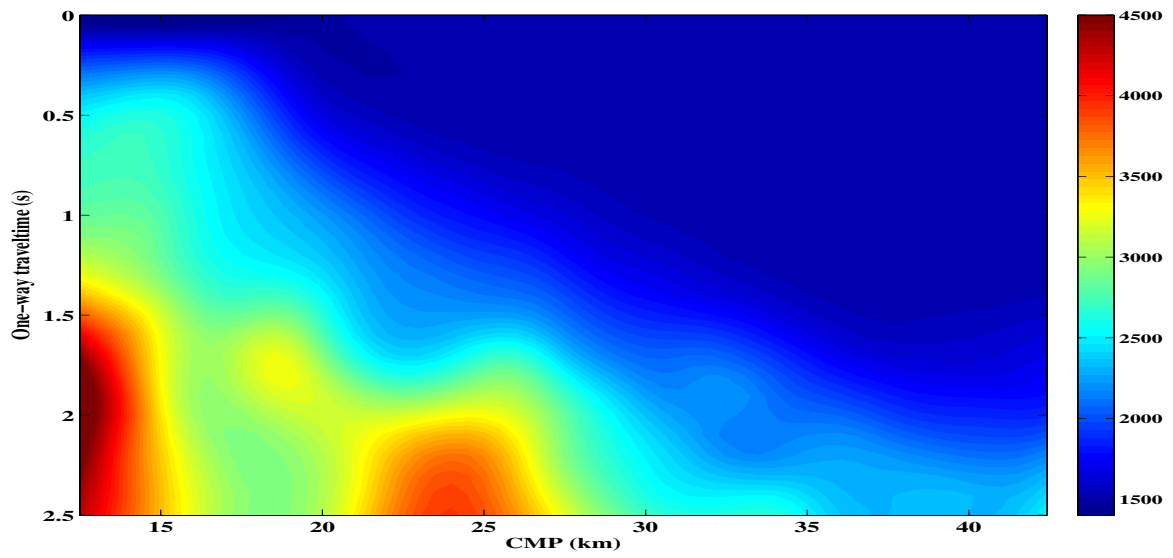
ACKNOWLEDGEMENTS

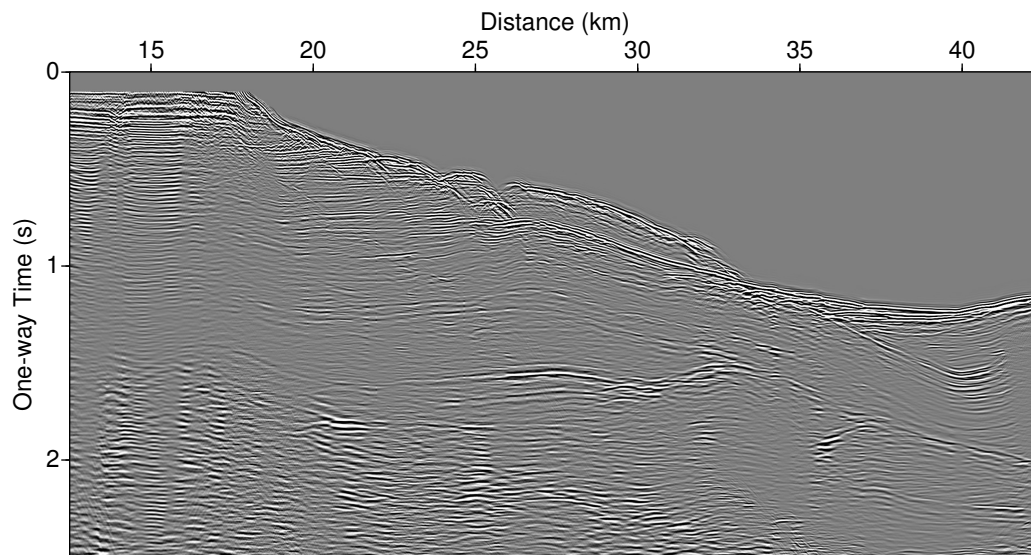**Figure 7:** Velocity model after smoothing with intermediate regularisation.

Figure 8: Time-migration with intermediately regularised velocity model.
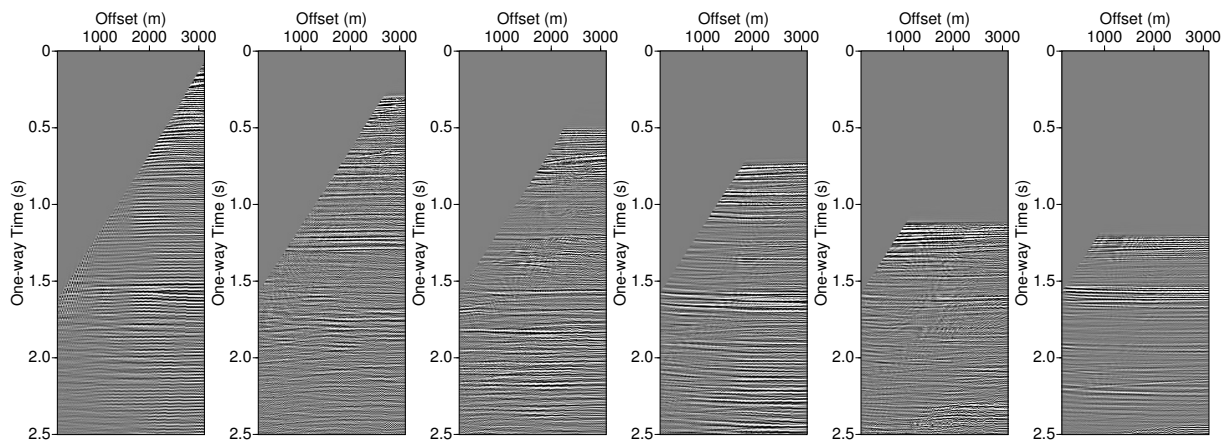

Figure 9: Time-migration common-image gathers with intermediately regularised velocity model.
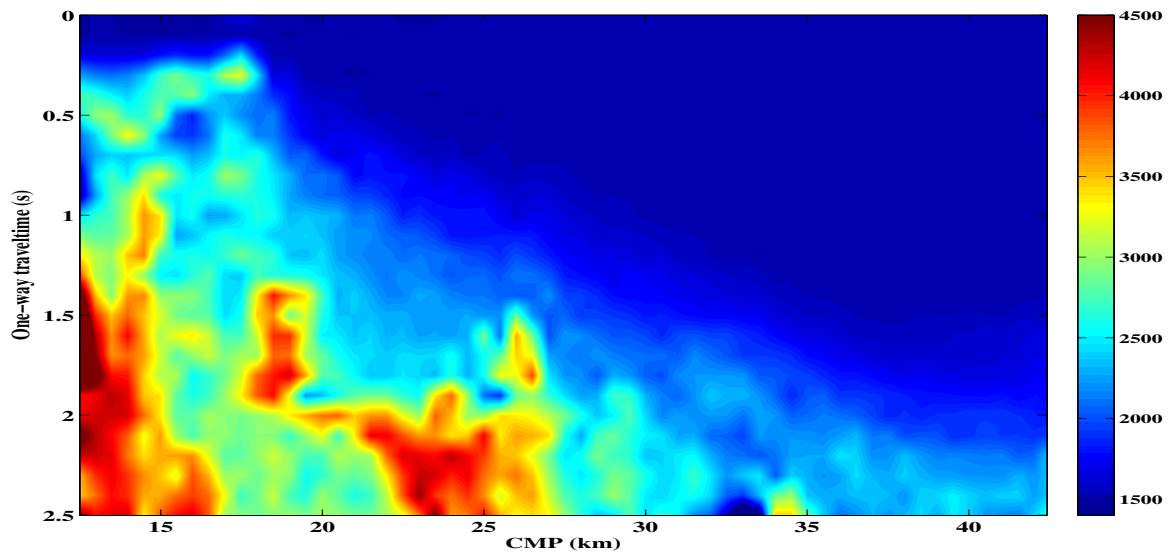
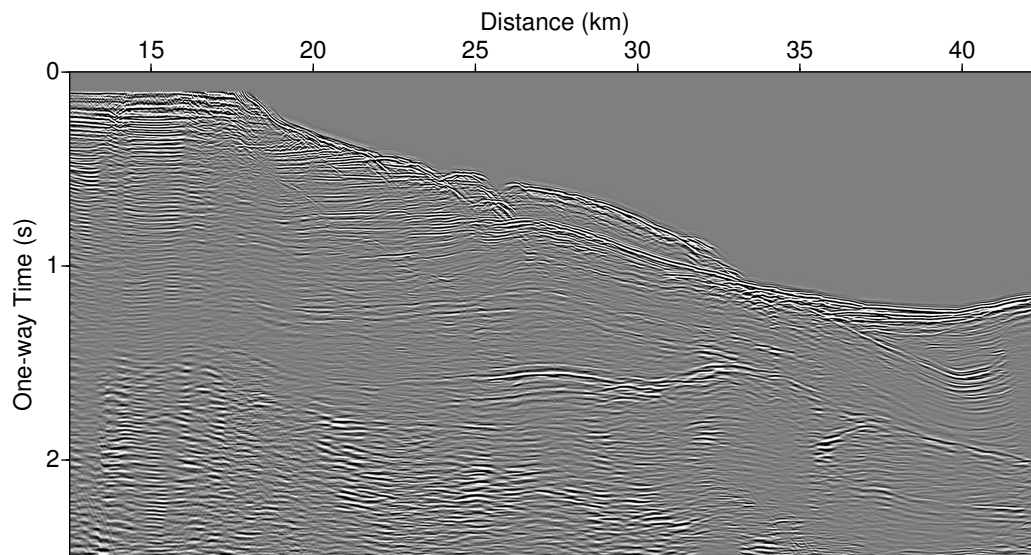**Figure 10:** Velocity model after smoothing with weak regularisation.

Figure 11: Time-migration with weakly regularised velocity model.
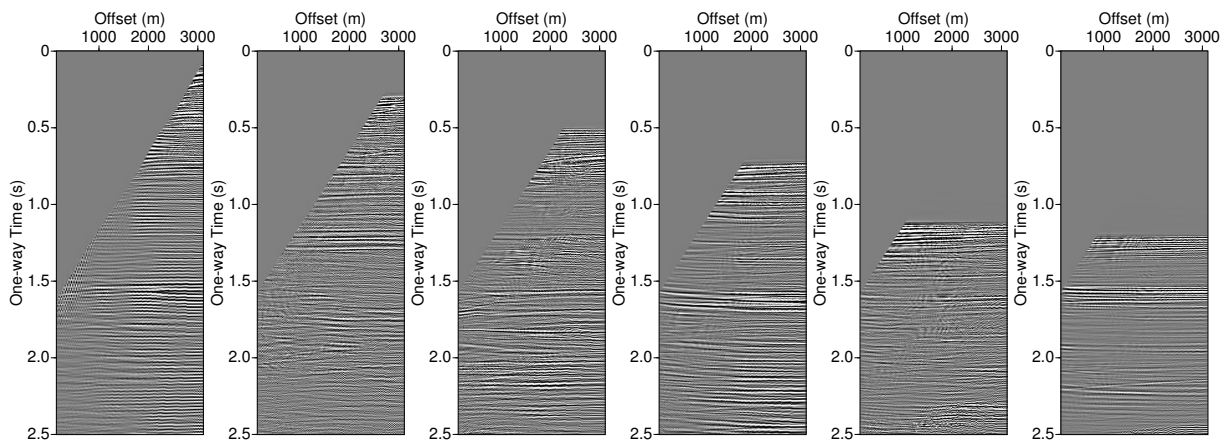

Figure 12: Time-migration common-image gathers with weakly regularised velocity model.

REFERENCES

Anikiev, D., Vanelle, C., Gajewski, D. Kashtan, B., and Tessmer, E. (2007). Localisation of seismic events by a modified diffraction stack. *Annual WIT Report*, 11:19–31.

Bleistein, N. (1987). On the imaging of reflectors in the earth. *Geophysics*, 52(7):931–942.

Erdélyi, A. (1956). *Asymptotic Expansions*. Dover Publications, New York.

Hertweck, T., Schleicher, J., and Mann, J. (2007). Data stacking beyond CMP. 26(7):818–827.

Keydar, S. (2004). Homeomorphic imaging using path integrals. pages P078:1–4. EAGE.

Keydar, S., Shtivelman, V., Milkenberg, M., and Moser, T. J. (2008). 3D prestack time migration by multipath summation. pages P036:1–4. EAGE.

Landa, E. (2004). Imaging without a velocity model using pathâĂŘsummation approach. volume 23, pages 1818–1821.

Landa, E., Fomel, S., and Moser, T. J. (2006). Path-integral seismic imaging. *Geophysical Prospecting*, 54(5):491–503.

Landa, E., Reshef, M., and Khaidukov, V. (2005). Imaging without a velocity model by path-summation approach: This time in depth. pages P011:1–4. EAGE.

Schleicher, J. and Costa, J. C. (2008). Migration velocity analysis by double path-integral migration. *WIT consortium, Annual Report*, 12:146–158.

Schleicher, J., Costa, J. C., Santos, L. T., Novais, A., and Tygel, M. (2009). On the estimation of local slopes. 74(4):P25–P33.

Shtivelman, V. and Keydar, S. (2005). Imaging shallow subsurface inhomogeneities by 3D multipath diffraction summation. *First Break*, 23(1):39–42.

Tygel, M., Schleicher, J., Hubral, P., and Hanitzsch, C. (1993). Multiple weights in diffraction stack migration. *Geophysics*, 58(12):1820–1830.